

High-pressure properties of wurtzite- and rocksalt-type aluminum nitride

P. E. Van Camp, V. E. Van Doren, and J. T. Devreese*

University of Antwerp, Rijksuniversitair Centrum Antwerpen, Groenenborgerlaan 171, B-2020 Antwerpen, Belgium

(Received 1 April 1991)

Electronic and ground-state properties of both wurtzite- and rocksalt-structure AlN are evaluated in the local-density-functional formalism using nonlocal norm-conserving pseudopotentials. For the wurtzite structure we obtain $a=3.129$ Å and $c=4.988$ Å and an internal parameter of 0.3825, which deviates considerably from the ideal value. In the case of the rocksalt structure we get $a=4.032$ Å. Both modifications are large-band-gap semiconductors with a direct gap in the wurtzite structure and an indirect gap in the rocksalt structure. The transition pressure from hexagonal to cubic was calculated to be 12.9 GPa, in reasonable agreement with the experimental value.

At ambient conditions aluminum nitride crystallizes in the wurtzite structure (space group C_{6v}^4), which differs from the zinc-blende structure (space group T_d^2) mainly at the relative positions of the third neighbors and beyond. It is a tetrahedrally coordinated III-V compound possessing chemical bonds that can be regarded as partially ionic and partially covalent. AlN is a large-band-gap semiconductor (band gap of about 6.3 eV) and has recently been used as a ceramic substrate in thin-film devices. It also has a high thermal conductivity (greater than 100 W/mK) and a low thermal expansion coefficient, very close to that of silicon. Furthermore, it has a high electrical resistivity.

In analogy with other wurtzite III-V compounds, AlN

was expected to transform to a cubic metallic structure. It was predicted¹ that the high-pressure phase would be the metallic β -tin structure. Recently, however, it was shown experimentally² that there is a structural phase transformation between 14 and 16.5 GPa at about 1500°C to a semiconducting rocksalt structure. In the present work we investigate the ground-state properties of both the hexagonal and the cubic modifications of AlN.

The calculations are based on the local-density-functional formalism together with *ab initio* norm-

TABLE I. Calculated and experimental lattice parameters and bulk moduli.

	Calculation	Experiment
Wurtzite structure		
a (Å)	3.129	3.110 ^a
c (Å)	4.988	4.980 ^a
c/a	1.594	1.601 ^a
u	0.3825	0.3821 ^a
B_0 (GPa)	195.0	202.0 ^b
B'_0	3.74	
B''_0 (GPa ⁻¹)	-0.019	
B_{iso} (GPa)	209.0	
B_a (GPa)	317.0	
B_c (GPa)	407.0	
σ	-0.643	
Rocksalt structure		
a (Å)	4.0316	4.045 ^c
B_0 (GPa)	215.0	
B'_0	4.58	
B''_0 (GPa ⁻¹)	-0.022	

^aReference 6.

^bReference 7.

^cReference 2.

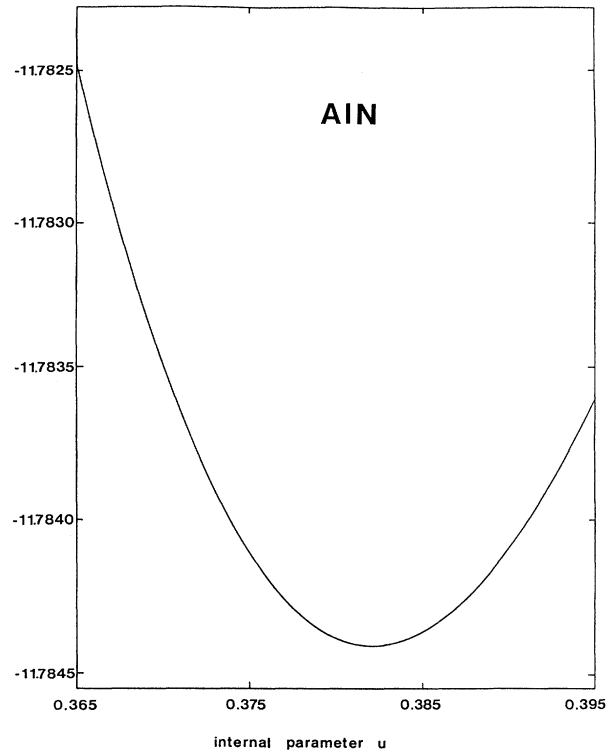


FIG. 1. Total energy (in Ry/atom) vs the internal parameter u for hexagonal AlN.

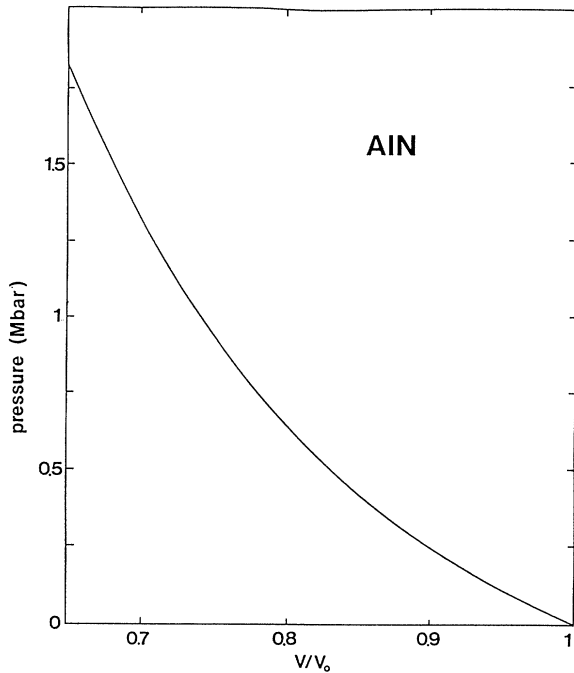


FIG. 2. Pressure (in Mbar) vs the reduced volume for hexagonal AlN.

conserving pseudopotentials.³ The accuracy of this method has been demonstrated before for a variety of solids. The Kohn-Sham equations are solved using a plane-wave basis with a kinetic-energy cutoff of 30 Ry. In the wurtzite structure the corresponding Hamiltonian matrix has a dimension of about 790. The number of \mathbf{k} points in an irreducible element of the Brillouin zone used in the calculation of the valence charge density is 6 and 10, respectively, for the wurtzite and rocksalt structure. For the exchange-correlation contribution the Wigner interpolation formula is employed.

For the ideal wurtzite structure we have $c/a = \sqrt{\frac{8}{3}} \approx 1.633$ and an internal parameter $u = \frac{3}{8}$. There are four atoms per unit cell. To determine the lattice parameters a , c , and u , the following procedure is used. At a chosen elementary cell volume V , and for

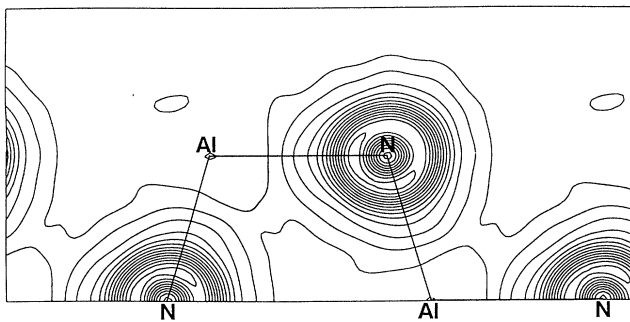


FIG. 3. Valence electronic charge density (in $e^-/\text{\AA}^3$) in the [110] plane of hexagonal AlN. The contour step is $0.2 e^-/\text{\AA}^3$.

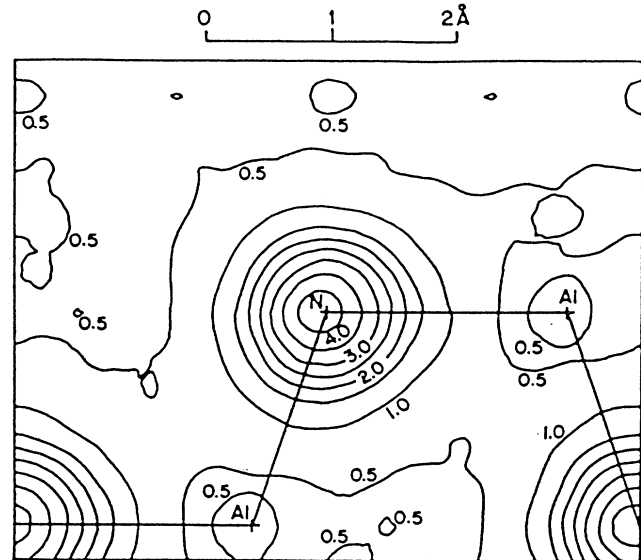


FIG. 4. Experimental valence charge density in the [110] plane of hexagonal AlN. The contour step is $0.5 e^-/\text{\AA}^3$ (taken from Ref. 10).

several values of a and c corresponding to V , the c/a ratio is determined by minimizing the total energy. This procedure is repeated for eight different volumes. Through these eight points the Birch equation of state⁴ is fitted leading to the equilibrium unit-cell volume V_0 , the bulk modulus for hydrostatic compression B_0 , and its first- and second-order pressure derivatives B'_0 and B''_0 . At the calculated volume V_0 , the internal parameter is determined by minimizing the total energy with respect to variations in u . The bulk modulus for ideal isotropic compression B_{iso} is obtained from the total energies calculated at a fixed c/a ratio. The linear bulk moduli for

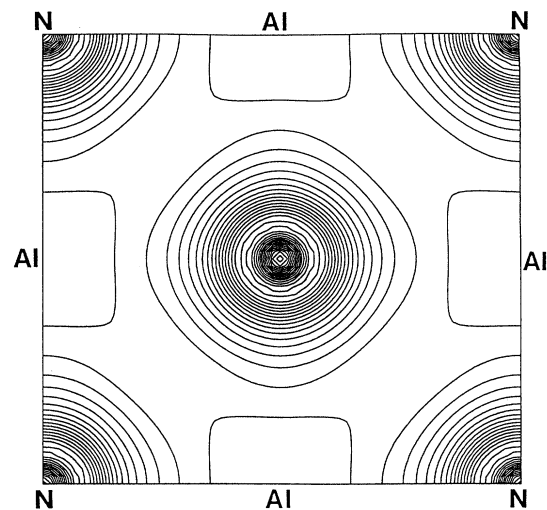


FIG. 5. Valence electronic charge density (in $e^-/\text{\AA}^3$) in the [100] plane of cubic AlN. The contour step is $0.2 e^-/\text{\AA}^3$.

compression along the a and c axes, B_a and B_c , respectively, are also derived from the total energies calculated above. The Poisson ratio σ , which is defined as the negative ratio of the transverse strain to the axial strain in a crystal subject to a uniaxial stress, is also determined. It should be noted that only two *ab initio* calculations on AlN were reported in the literature.⁵

In the rocksalt structure (space group O_h^5), AlN has only two atoms per unit cell. The same kinetic-energy cutoff (30 Ry) as above is used. Since there is only one lattice constant in this case, the total energy is evaluated at eight different unit-cell volumes. Again the Birch equation is used to fit these values. All the results regarding the lattice properties are given in Table I. The lattice parameters are in excellent agreement with the experimental values both for the wurtzite and rocksalt structures. The linear bulk moduli B_a and B_c are rather close together, indicating a relatively small anisotropy. In a strongly anisotropic crystal such as graphite, the ratio B_a/B_c is as high as 28.⁸ Another indication of small anisotropy is the fact that B_0 and B_{iso} are almost equal. Figure 1 shows the total energy as a function of the internal parameter u . As is often the case in the wurtzite structure,⁹ AlN also deviates considerably from the ideal arrangement. The empirical rule that only wurtzite structures with c/a ratios lower than the ideal value are stable is obeyed here. The fitted equation of state, using the Birch expression, is shown in Fig. 2.

Figure 3 displays the electronic valence charge density in the [110] plane of hexagonal AlN and should be compared with the experimental charge density taken from Ref. 10 and shown in Fig. 4. As expected, the agreement is quite good. The contours shown suggest that the bonding is more ionic than covalent. Similar conclusions were derived from the x-ray-diffraction experiment.¹⁰ Such bonds are often characterized by their ionicity, which ranges from 0 (fully covalent) to 1 (fully ionic). In order to establish a relation to, e.g., the Philips ionicity parameter, one possibility consists of transforming the wave functions to a localized basis and to project out the bonding and antibonding character.¹¹ The electronic valence

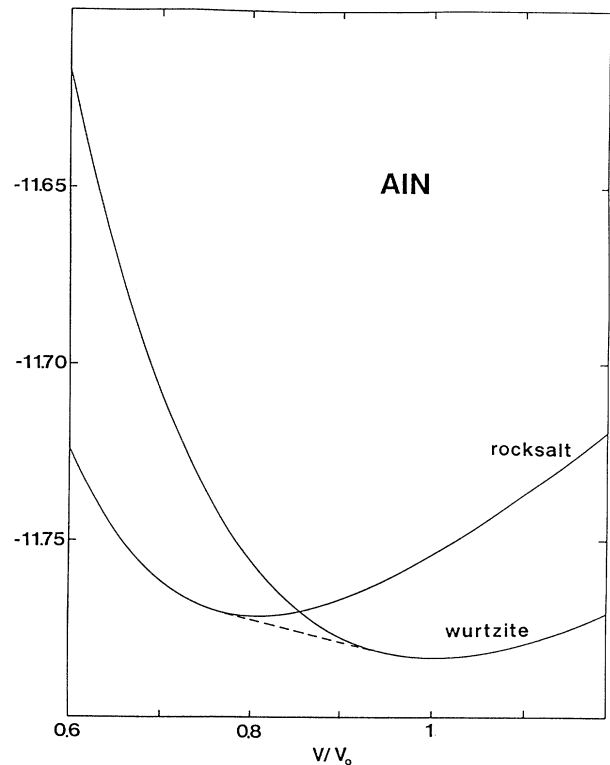


FIG. 6. Total energies (in Ry/atom) as a function of the reduced volume for hexagonal and cubic AlN. The dashed line is the common tangent of the two curves and indicates the path of the pressure-induced phase transition.

charge density in the [100] plane of cubic AlN is shown in Fig. 5. It clearly illustrates the picture of ionic bonding, i.e., an almost spherical charge distribution around the anion. In both cases the N charge is more spread out, while the Al charge is much more concentrated on the Al sites. Due to the larger number of valence electrons originating from the N atoms, most contours are concentrated around the N sites. Figure 6 shows the total energies

TABLE II. Conduction-band energies (with respect to the top valence band at Γ) and their first- and second-order pressure derivatives.

	E (eV)	$\frac{dE}{dp}$ (meV/GPa)	$\frac{d^2E}{dp^2}$ (meV/GPa ²)
Wurtzite structure			
Γ	3.09	36.3	-0.18
K	4.36	-6.4	0.18
L	4.59	8.2	0.072
M	4.93	7.7	0.11
A	5.57	35.7	-0.16
H	7.14	8.1	0.10
Rocksalt structure			
X	4.04	35.0	-2.83
Γ	4.99	63.2	-0.60
L	5.52	24.9	-0.14

of both hexagonal and cubic AlN as a function of the reduced volume. The slope of the dashed line is the pressure at which the two phases coexist. For this pressure we find 12.9 GPa. The experimental value is situated between 14.0 and 16.5 GPa (at about 1500 °C).² It must be noted that the calculated transition pressure is very sensitive to the difference in total energies of the two phases. Therefore these energies should be calculated to the same accuracy, which is hard to accomplish due to the different number of integration points over the Brillouin zone. The number of points is determined by the symmetry of the zone. The structural phase transformation is accompanied with a rather large volume contraction. The calculated value of this contraction is 22.5% while experimentally one found 20.6%.²

At the calculated lattice parameters, the band structures of both hexagonal and cubic AlN are evaluated. Hexagonal AlN is a direct-gap semiconductor with a calculated energy gap at the Γ point of 3.09 eV. This is

about 50% less than the measured value of 6.3 eV.¹² This large difference is to be expected and is characteristic for LDA calculations. It can be remedied using a nonlocal energy-dependent electron self-energy operator as shown in Ref. 13. Nevertheless the LDA values of the pressure derivatives turn out to be accurate.¹⁴ These are shown in Table II together with the band gaps relative to the top of the valence band at Γ . To our knowledge no experimental values have been published. Cubic AlN turns out to be a semiconductor with an indirect band gap (at the X point) of 4.04 eV.

This work was performed in the framework of the Institute for Materials Science (IMS) of the University of Antwerp (RUCA and UIA) funded by the IUAP 11 (Interuniversitaire Attractiepool 11 "Materials Science") of the Belgian Ministry of Scientific Affairs. Supercomputer time was provided by the NFWO-Supercomputer Project of the Belgian National Science Foundation.

*Also at University of Antwerp (UIA), Universiteitsplein 1, B-2610 Wilrijk, Belgium, and Eindhoven University of Technology, P.O. Box 513, NL-5600 MB Eindhoven, The Netherlands.

¹J. Van Vechten, Phys. Rev. **178**, 1479 (1973).

²H. Vollstädt, E. Ito, M. Akaishi, S. Akimoto, and O. Fukunaga, Proc. Jpn. Acad. B **66**, 7 (1990).

³See, e.g., *Electronic Structure, Dynamics and Quantum Structural Properties of Condensed Matter*, edited by J. T. Devreese and P. E. Van Camp (Plenum, New York, 1985).

⁴F. Birch, J. Geophys. Res. **83**, 1257 (1978).

⁵W. Ching and B. Harmon, Phys. Rev. B **34**, 5305 (1986); N. Christensen (unpublished).

⁶H. Schulz and K. Thiemann, Solid State Commun. **23**, 815 (1977).

⁷K. Tsubouchi, K. Sugai, and N. Mikoshiba, in *1981 Ultrasonic Symposium Proceedings* (IEEE, New York, 1981), p. 375.

⁸O. Blackslee, D. Proctor, E. Seldin, B. Spence, and T. Weng, J. Appl. Phys. **41**, 3373 (1970).

⁹R. Wyckoff, *Crystal Structures*, Vol. 1 (Wiley, New York, 1965).

¹⁰E. Gabe, Y. Le Page, and S. Mair, Phys. Rev. B **24**, 5634 (1981).

¹¹N. Christensen, S. Satpathy, and Z. Pawlowska, Phys. Rev. B **36**, 1032 (1987).

¹²B. Perry and R. Rutz, Appl. Phys. Lett. **33**, 319 (1978).

¹³M. Hybertsen and S. Louie, Phys. Rev. Lett. **55**, 1418 (1985); Phys. Rev. B **34**, 5390 (1986).

¹⁴X. Zhu, S. Fahy, and S. Louie, Phys. Rev. B **39**, 7840 (1989); **39**, 5821 (1989).